Electronic Supplementary Material (ESI) for Nanoscale.
This journal is © The Royal Society of Chemistry 2019

Supporting Information

Ultra-sharp and surfactant-free silver nanowire for scanning tunneling microscopy and tip-enhanced Raman spectroscopy

Qiushi Liu[*1], Sanggon Kim*[*2], Xuezhi Ma[1], Ning Yu[2], Yangzhi Zhu[2], Siyu Deng[1], Ruoxue Yan[2,3], Huijuan Zhao[4], Ming Liu[1,3]*

Addresses:

[1]Department of Electrical and Computer Engineering, Bourns College of Engineering, University of California-Riverside, Riverside, California 92521, United States

[2]Department of Chemical and Environmental Engineering, Bourns College of Engineering, University of California-Riverside, Riverside, California 92521, United States

[3]Material Science Engineering program, Bourns College of Engineering, University of California-Riverside, Riverside, California 92521, United States

[4]Department of Mechanical Engineering, Clemson University, Clemson, SC 29634-0921, United States

*These authors contribute equally

Correspondence and requests for materials should be addressed to M.L. (email: mingliu@ucr.edu) and R.Y. (email:rxyan@engr.ucr.edu)

1. PVP removal from the AgNW tip region

Figure 2 shows the removal of PVP molecules from the AgNW sidewalls. Sidewalls were chosen to show the removal performance because it is known that PVP has higher binding energy with the sidewall {100} than the tip {111}[1, 2]. During the $NaBH_4$ bubbling treatment, the PVP at the AgNW tips are also efficiently removed. Figure S1a and b show the comparison of two AgNWs, without and with the $NaBH_4$ PVP-removal treatment, respectively.

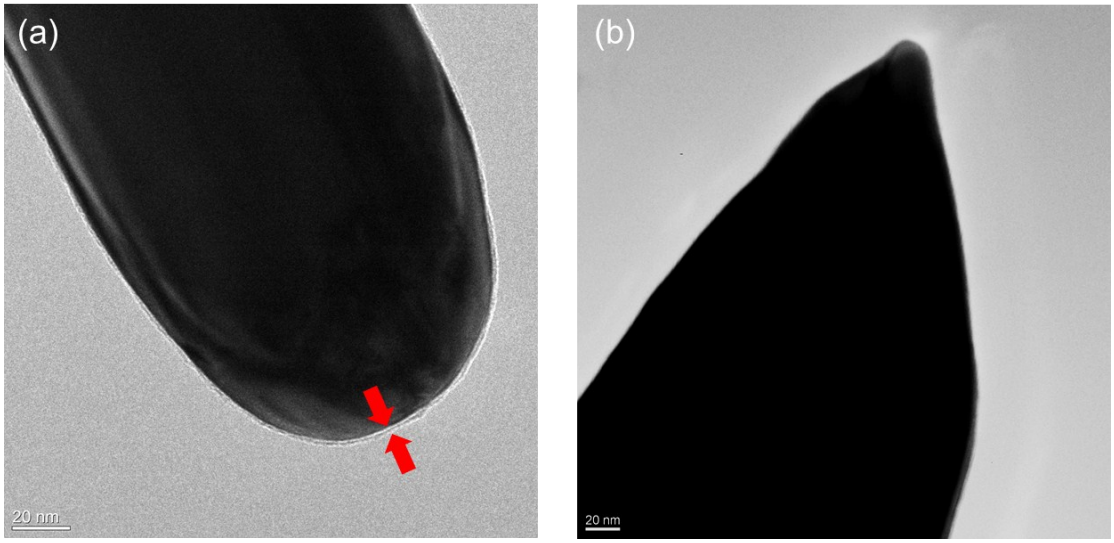

Figure S1. TEM images of the AgNW tips without (a) and with (b) the PVP removal treatment.

2. Influence of PVP to the STM performance

The influence of PVP layer on AgNW surface to the STM scanning results is shown in Figure 2. On the other hand, the PVP layer can also hinder the probe launching process, in particular with certain launching parameters, such as low bias voltage (<1V) and high tunneling-current setpoint (e.g. nA). Figure S2b shows the probe launching process with -0.5V probe voltage and 1nA target current, monitored by a high-magnification long-working-distance objective lens (Figure S2a). When the AgNW tip apex touches the Au substrate, the thin PVP layer reduces the tunneling current, resulting in the failure in triggering the abortion program to stop the probe approaching. As a result, the probe keeps approaching the substrate and bending the AgNW, until the Pt/Ir probe touches the substrate.

High bias voltage (Figure S2c, -1.5V) is sufficient for the probe launching process. However, even in this case, the long-chain PVP molecules at AgNW apex, despite multiple ethanol washing cycles, could not be removed by the high-voltage-pulse cleaning procedure, a cleaning method commonly used to remove molecules from STM probe tips, and the scanned images are similar in quality to Figure 2c-iii.

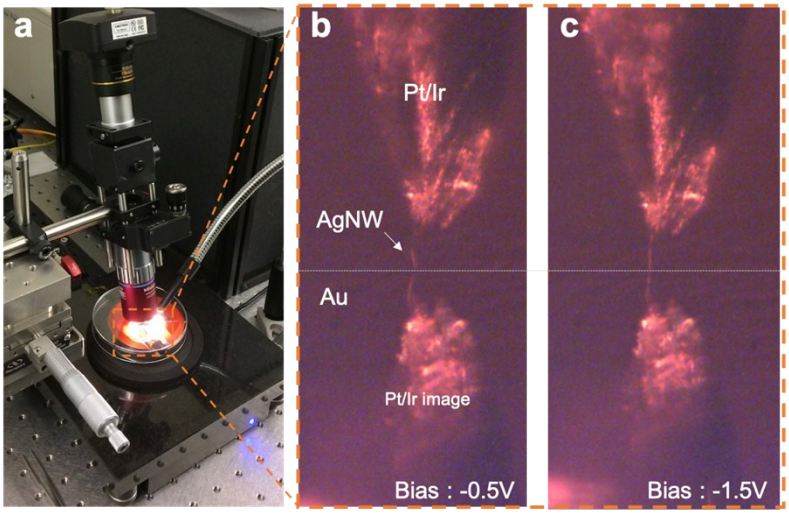

Figure S2 | The influence of PVP residues to the AgNW probe launching. a, The STM integrated with a long-working-distance objective lens for the monitor of the AgNW morphology during the STM probe launching. **b**, With low bias voltage (-0.5V on AgNW), the Pt/Ir probe kept moving towards the substrate, even after the AgNW tip apex touched the Au substrate, leading to a bent AgNW. **c**, With a higher bias voltage (-1.5V), the AgNW probe can be launched onto the Au substrate. However, the STM image quality is poor. The AgNW used here was pretreated 6 cycles of ethanol wash.

3. Influence from AgNW oxidation to the STM performance

The native oxide (Ag_2O) on silver exposed to the natural oxygen environment can quickly reach ~10 Å in thickness[3]. Ag_2O has a high electrical resistivity around 10^8 ohm · cm [4] and a bandgap around 1.5 eV [5], both of which prevent the tunneling current and restrict the STM performance. Therefore, although we do not observe any noticeable change in TEM (the TEM contrast of Ag and Ag_2O are very similar) between a freshly-prepared PVP-removed AgNW (Figure S3c) and a PVP-free AgNW that has been stored in air for 24 hrs (Figure S3d), we did see that the native oxide has a drastically influence the STM imaging quality. As displayed in Figure S3a, a fresh STM probe (within 10 mins of air exposure) could form clear image of the cluster morphology of the Au substrate. However, after exposed to the air for 2 hours, the oxidation layer on the AgNW surface impeded the tunneling current which results in the smeared STM image Figure S3b. Therefore, the AgNW-STM probe needs to be operated in inert gas environment or in vacuum, to prevent the oxidization.

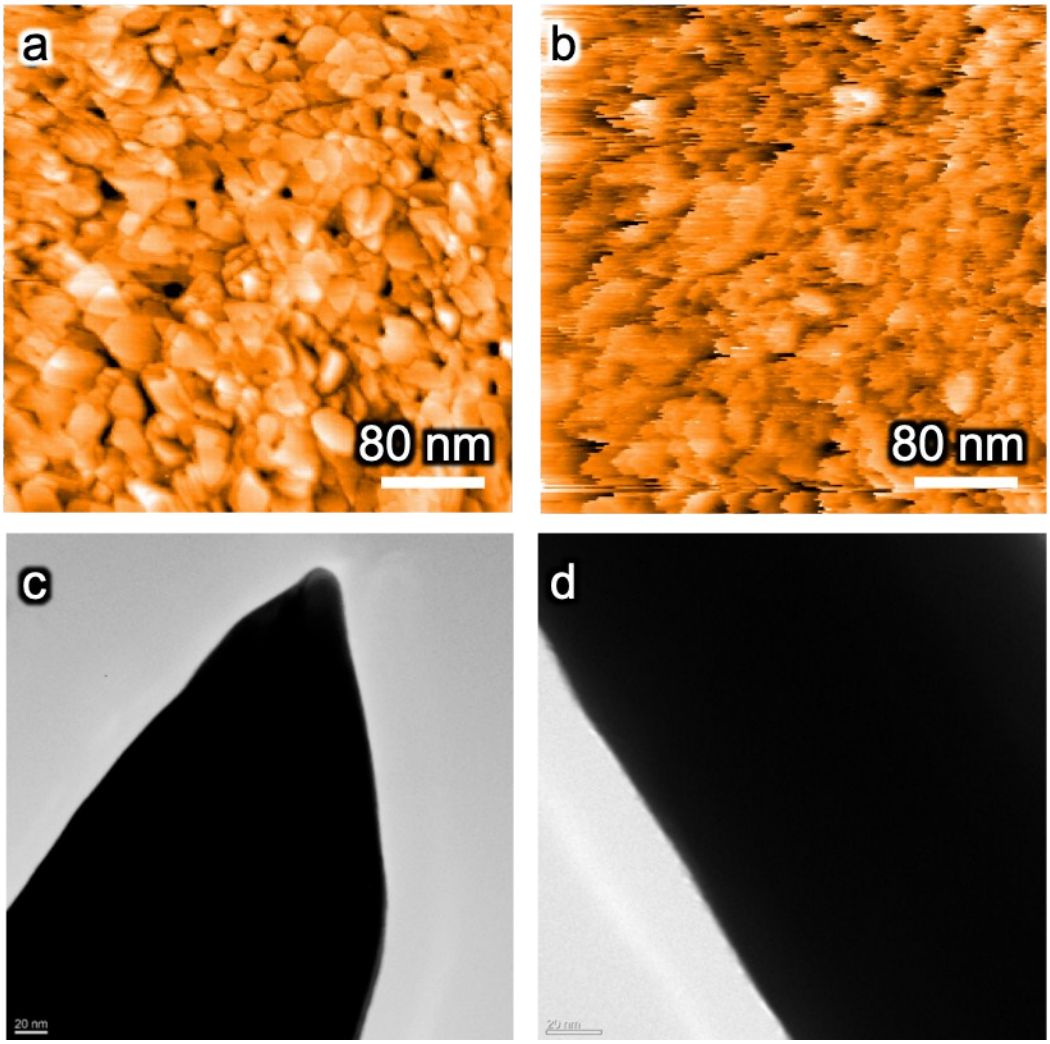

Figure S3 Oxidation of AgNW and its influence to STM imaging. **a**, STM image of a Au substrate, obtained by a freshly-prepared AgNW probe. **b**, The STM image acquired by the same probe after exposed to air for 2 hrs. **c**, TEM image of a freshly-cleaned AgNW. **d**, A PVP-removed AgNW, after stored in air for 24 hrs.

4. Influence of Tip radius to the STM performance

The regular AgNWs with large tip radii have a higher chance for the multiple-tunneling-channel effect, which not only smear spatial details, but also create ghost images. This effect can be seen in Figure S4a, which is an STM image of a gold surface scanned by a round-tip AgNW probe. The ghosting effect, as highlighted by the red rectangular, indicates that there are at least 3 tunneling channels that outline the same feature repeatedly. The estimated distance between channels is

around 10~20 nm, which is within the range of the tip radius of a flat tip, as shown in Figure S4b and c. The red arrows point to the possible locations of the multiple tunneling channels.

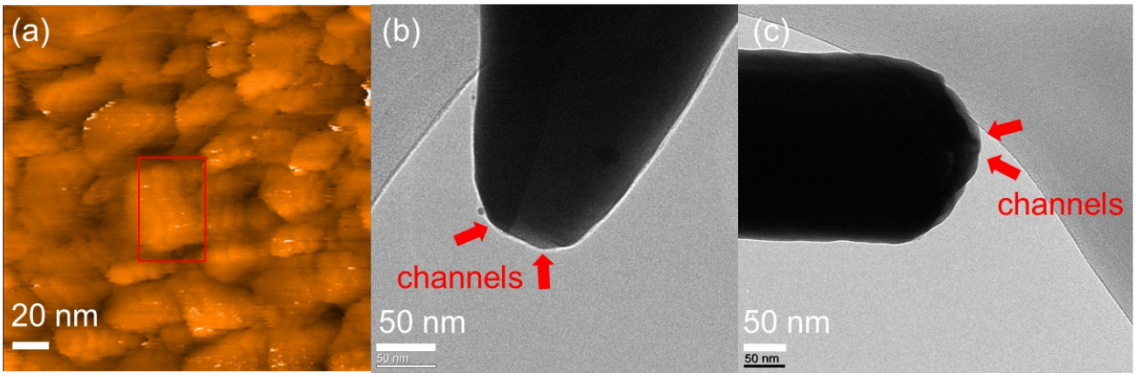

Figure S4. (a) STM result whose ghost comes from multi tunneling channels. (b) and (c) shows potential channels from round AgNW tip.

5. Repeatability of the TERS performance

In order to gain insights into the influence of the AgNW tip shape to the TERS experiment, five sharp-tip and five round-tip AgNWs have been tested. The measurements were conducted with contact-mode AFM (AgNW directly mounted on the cantilever). A monolayer graphene on 30 nm ultra-flat silver substrate was used as the evaluation sample. The TERS experiments were carried out using the same setup and parameters as described in the manuscript. A 532 nm green laser (~2 mW at the sample surface) is focused at the probe apex through a long-working-distance objective lens (NA=0.6). Both the sharp-tip and round-tip AgNWs were thoroughly cleaned through the $NaBH_4$ bubbling method, and the TERS experiments were conducted within 30 mins after the probe preparation to avoid oxidization.

The Raman signals from the graphene monolayer have been measured for each probe at ~5 different positions, with typical spectra shown in Figure S5a and c, for sharp-tip and round-tip probes, respectively. Figure S5b and d show the statistic of the 2D peak intensity measured with each probe for the sharp and the round tip AgNW probes respectively, with the standard errors indicated by the error bar and the original data listed in Table 1. Overall, the sharp-tip AgNW shows ~1480±140 counts, while the regular round tip probe shows 530±100 counts.

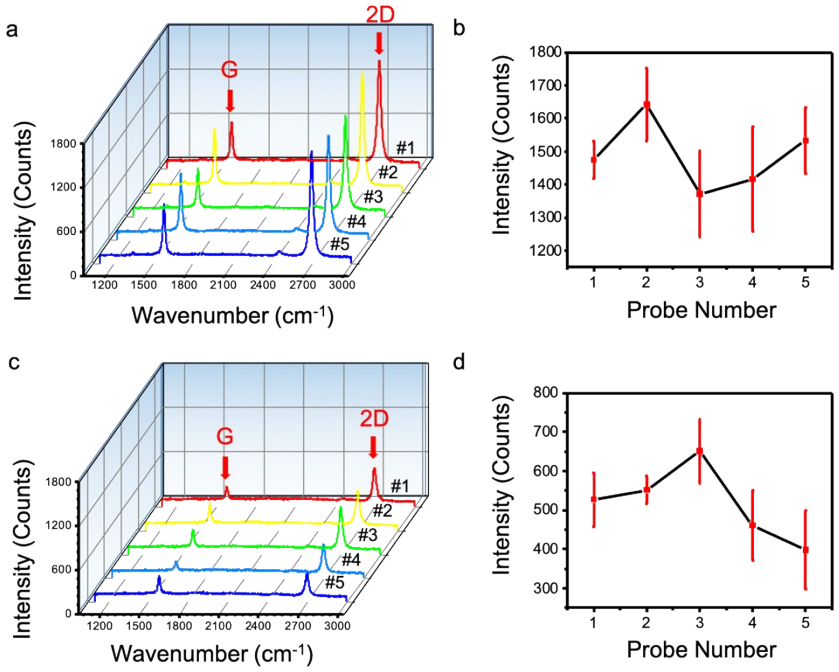

Figure S5. Monolayer Graphene Raman signal using (a) five sharp tip and (c) five round tip. (b) and (d) show each individual probe's 2D peak intensity distribution at different positions for sharp and round tips. Acquisition time = 3 sec

Table 1 Data from individual TERS probes (2D peak height in counts)

Location	Sharp#1	Sharp#2	Sharp#3	Sharp#4	Sharp#5	Rounded #1	Rounded #2	Rounded #3	Rounded #4	Rounded #5
1	1532.7	1774.9	1372.0	1306.0	1384.1	624.1	551.3	653.8	460.5	353.3
2	1520.8	1507.3	1622.2	1659.3	1532.6	526.7	625.1	692.7	421.0	398.1
3	1395.0	1642.0	1329.0	1416.3	1463.8	512.1	605.7	464.6	588.5	343.9
4	1424.1	1696.6	1328.7	1316.2	1592.7	542.0	587.5	651.1	563.1	560.1
5	1474.9	1542.0	1306.0	1264.1	1632.6	441.4	538.8	560.5	405.3	484.1
Stat.	1470 ± 60	1632 ± 110	1390 ± 130	1390 ± 160	1520 ± 100	530 ± 60	581 ± 36	600 ± 90	490 ± 80	430 ± 90

References:

1. Sun, Y., Gates, B., Mayers, B. & Xia, Y. Crystalline silver nanowires by soft solution processing. *Nano letters* **2**, 165-168 (2002).

2. Al-Saidi, W., Feng, H. & Fichthorn, K.A. Adsorption of polyvinylpyrrolidone on Ag surfaces: insight into a structure-directing agent. *Nano letters* **12**, 997-1001 (2012).

3. De Rooij, A. The oxidation of silver by atomic oxygen. *EsA Journal* **13**, 363-382 (1989).

4. Tvarusko, A. The electric resistivity of Ago. *Journal of the Electrochemical Society* **115**, 1105-1110 (1968).

5. Fortin, E. & Weichman, F. Photoconductivity in Ag2O. *physica status solidi (b)* **5**, 515-519 (1964).